

Hadronic Final States in Deeply Inelastic Scattering *

M. Kuhlen

Max-Planck-Institut für Physik
Werner-Heisenberg-Institut
Föhringer Ring 6
D-80805 München
Germany
E-mail: kuhlen@desy.de

Abstract

Results on hadronic final states in deeply inelastic scattering are reviewed. They comprise jet production and its interpretation in perturbative QCD, signatures to distinguish conventional QCD dynamics from possible new features of QCD at small x , and measurements of inclusive charged particle production. Theoretical developments such as color dipole emission and instanton induced final states are reported on.

1. Introduction

The basic measurement in deeply inelastic scattering (DIS) is a measurement of the cross section $ep \rightarrow eH$ in terms of the structure function F_2 , where H stands for any hadronic system. A wealth of information upon the partonic structure of the proton and its dynamics have been obtained from structure function measurements. Measurements of the properties of the hadronic final state H provide complementary information which cannot be obtained from inclusive structure functions.

In the simple quark parton model (QPM) of DIS, a quark is scattered out of the proton by the virtual boson

emitted from the scattering lepton. QCD modifies this picture. Partons may be radiated before and after the boson-quark vertex, and the boson may also fuse with a gluon inside the proton by producing a quark-antiquark pair (figure 1). In fact, the parton which is probed by the boson may be the end point in a whole cascade of parton branchings. This parton shower materializes in the hadronic final state, allowing experimental access to the dynamics governing the cascade.

HERA has opened a new kinematic domain to study QCD in DIS, and most contributions in this working group were concerned with HERA physics. In HERA electrons of $E_e \approx 27$ GeV collide with protons of $E_p = 820$ GeV, resulting in a centre of mass energy of $\sqrt{s} \approx 300$ GeV. The kinematic region covered with the present data is roughly $10^{-4} < x < 10^{-1}$, $7 \text{ GeV}^2 <$

* Summary talk from the working group II "Hadronic Final States" at the Workshop on Deep Inelastic Scattering and QCD, Paris, April 1995

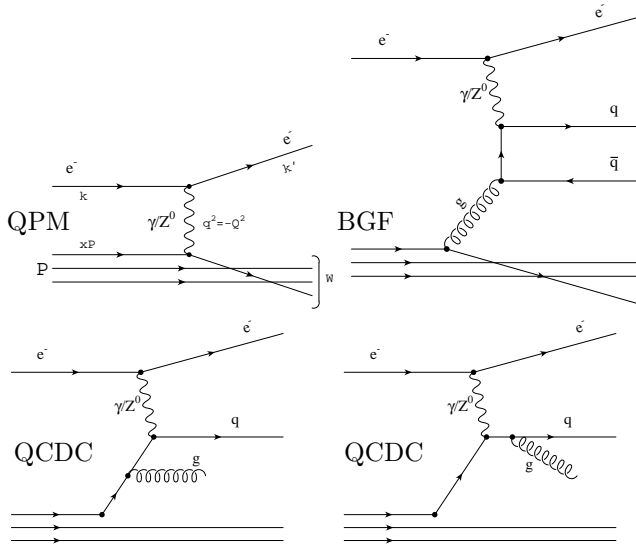


Figure 1. Diagrams for DIS in $O(\alpha_s^0)$ (quark parton model - QPM) and in $O(\alpha_s^1)$: boson-gluon fusion (BGF) and QCD Compton (QCDC) processes.

$Q^2 < 5000 \text{ GeV}^2$ and $40 \text{ GeV} < W < 300 \text{ GeV}$, where W is the invariant mass of the hadronic system, Q^2 the negative 4-momentum transfer squared, and x the Bjorken scaling variable, to be identified with the proton momentum fraction carried by the scattering parton. HERA offers the opportunity to study the evolution of physics quantities over a large kinematic range. The large phase space available for hard QCD radiation, which can be treated in perturbative QCD, leads to prominent jets observable in the final state. Another area of recent interest is the kinematic regime at small x ($x \lesssim 10^{-3}$) but sizeable Q^2 , not accessible at pre-HERA DIS experiments, where novel QCD dynamics are expected to play a rôle (e.g. [1]).

The two HERA detectors ZEUS and H1 [2] are large multipurpose, “almost 4π ” detectors built around the beam line. Inner tracking detectors for charged particle detection are surrounded by a magnet and calorimetry. Both the scattered electron serving as a tag for DIS events and the hadronic final state are measured. Note that a substantial part of the hadronic final state, the proton remnant, leaves the detectors unobserved in the beam pipe. The region close to the proton beam direction is often referred to as the forward region.

Apart from the laboratory frame, the hadronic centre of mass system (CMS) and the Breit frame are used in the analyses. The Breit frame is defined by the condition that the virtual photon does not transfer energy, only momentum. In the QPM picture the scattering quark would thus just reverse its momentum of magnitude $Q/2$. The CMS is defined as the centre of mass system of the incoming proton and the virtual boson, i.e. the CMS of the hadronic final state with

invariant mass W . In both systems the hemisphere defined by the virtual photon direction is referred to as the current region, the other (containing the proton remnant) as the target region. The CMS current and target systems are back to back with momentum $W/2$ each. Longitudinal and transverse quantities are calculated w.r.t. the boson direction. With a longitudinal boost from the Breit frame into the CMS, particles formerly assigned to the target hemisphere may now end up in the current hemisphere.

Monte Carlo (MC) models based upon QCD phenomenology are used to simulate the DIS process. The MEPS model (Matrix Element plus Parton Shower), an option of the LEPTO generator [3], incorporates the QCD matrix elements up to first order, with additional soft emissions generated by adding leading log parton showers. In the colour dipole model (CDM) [4, 5] radiation stems from a chain of independently radiating dipoles formed by the colour charges. Both programs use the Lund string model [6] for hadronizing the partonic final state. Deficiencies of the Herwig parton shower model [7] have now been fixed by adding matrix element corrections [8, 9]. This model implements an alternative (cluster) fragmentation scheme [10], allowing for valuable cross checks in the future.

2. Jet physics

The processes contributing to DIS up to first order in α_s are shown in figure 1. The QPM process results in a so-called “1+1” jet topology, while the QCDC and BGF processes give “2+1” jet events, where the “+1” refers to the unobserved remnant jet. From a measurement of the 2+1 jet rate at large x and Q^2 , where the parton densities are well known, α_s can be measured. At small x and Q^2 , one can determine the largely unknown gluon density from the rate of 2+1 jet events, which is then dominated by the BGF graph (assuming α_s to be known). Complications arise from the fact that the initial state contains strongly interacting particles, leading to the evolution of parton showers. Such effects need to be taken into account with the help of MC simulations.

2.1. The strong coupling constant α_s

Both H1 and ZEUS use the modified JADE algorithm [11] with resolution parameter $y_{\text{cut}} = 0.02$ to define jets in the α_s analysis. A pseudoparticle is introduced to account for the unobserved remnant, and then all particles i, j satisfying $m_{ij}^2 < y_{\text{cut}} \cdot W^2$ are merged into jets. The chosen y_{cut} value is a compromise between statistical precision (small y_{cut}), and controllable higher order corrections (large y_{cut}) [12]. In the H1 analysis

[13] an angular cut $\theta_{\text{jet}} > 10^\circ$ (w.r.t. the proton direction) protects against parton showers close to the remnant. The obtained jet rates are corrected for detector effects, remaining parton shower contributions and hadronization with the MEPS model. In order to extract α_s from the measured jet rates, it is important to take next to leading order (NLO) corrections into account to reduce dependencies upon y_{cut} and the chosen renormalization and factorization scales [12]. Using PROJET [14] as NLO calculation, the measured jet rate then yields measurements of $\alpha_s(Q^2)$ in the range $10 \text{ GeV}^2 < Q^2 < 3000 \text{ GeV}^2$, which can be seen to run according to the QCD expectation [13]. However, below $Q^2 = 100 \text{ GeV}^2$, the corrections are very model dependent (MEPS vs. CDM). Therefore only data at $Q^2 > 100 \text{ GeV}^2$ are used to extract $\alpha_s(m_Z^2) = 0.123 \pm 0.018$ [13].

For 2+1 jet events with $Q^2 > 160 \text{ GeV}^2$ and $x > 0.01$, ZEUS has measured the jet distribution in the Lorentz invariant z_p variable [15], which in the centre of mass frame of the virtual photon and the incoming parton is an angular variable $z_p = \frac{1}{2} \cdot (1 - \cos \hat{\theta}_{\text{jet}})$. Here $\hat{\theta}_{\text{jet}}$ is the angle of the jet w.r.t. the direction of the incoming parton. Perturbation theory in next to leading order (NLO) [14] is able to describe the jet angular distribution down to $z_p \approx 0.1$. For $z_p < 0.1$ an excess of jets is observed. Both, the MEPS (LO matrix element + parton showers) and ME (pure LO matrix element) simulations are similar to the NLO calculation [15]. The excess of jets at $z_p < 0.1$ is therefore unlikely to be cured by next to NLO calculations.

For the α_s extraction, a cut $z_p > 0.1$ restricts the data to a region well described by NLO perturbation theory and QCD models [16]. The preliminary α_s measurements [16] for $100 \text{ GeV}^2 \lesssim Q^2 \lesssim 3600 \text{ GeV}^2$ demonstrate the potential of HERA to study the dependence of α_s upon the renormalization scale, and agree well with the QCD expectation (see figure 2). It is expected that already the analysis of the 1994 HERA data, once finalized, will yield a very competitive measurement of $\alpha_s(m_Z^2)$.

2.2. The gluon density in the proton

The 2+1 jet sample (defined with the cone algorithm in the CMS) in the range $10 \text{ GeV}^2 < Q^2 < 100 \text{ GeV}^2$ is used to extract the gluon density $g(x_g, Q^2)$, because there the BGF graph (figure 1) dominates (BGF:QCDC $\approx 4:1$ [16, 17]). The momentum fraction x_g which the gluon carries is calculated from the invariant mass \hat{s} of the hard subsystem forming the 2 jets via $x_g = x(1 + \hat{s}/Q^2) \approx \hat{s}/W^2$. Special cuts remove events affected by parton showers [16, 17]. The MEPS model is used to unfold detector effects, the QCDC contribution, QPM background and remaining parton shower contributions.

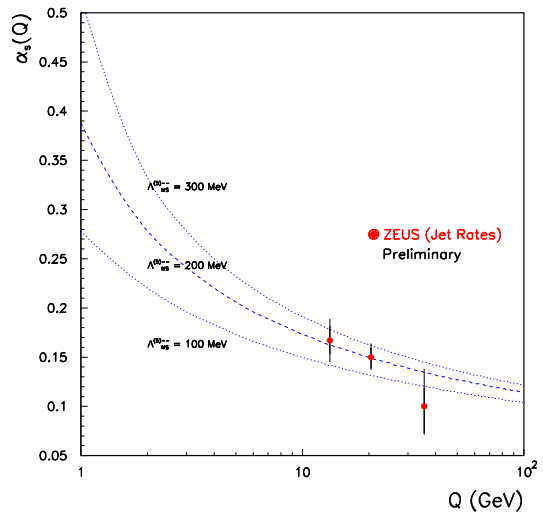


Figure 2. Preliminary $\alpha_s(Q)$ measurements from ZEUS, compared to the QCD predictions corresponding to $\Lambda_{\overline{\text{MS}}} = 100, 200$ and 300 GeV .

The MEPS model employs a cut-off for invariant parton-parton masses $m_{ij}^2 > y_{\text{min}} \cdot W^2$ to regulate divergencies of its LO matrix element. In order to access x_g as small as possible, \hat{s} is chosen as small as experimental resolution allows, and as problems with the diverging LO matrix element can be avoided. It has to be ensured that the BGF events to be analyzed are actually generated by the model and do not fall below that cut-off [16, 17].

The H1 analysis [16] uses a fixed cut-off $\hat{s} > 100 \text{ GeV}^2$ to define BGF events, and they parametrize the MEPS cut-off such as to follow the limit at which the order α_s contribution exceeds the total cross section within a margin of $\Delta\sqrt{\hat{s}} = 2 \text{ GeV}$. ZEUS uses the standard y_{min} cut-off scheme in the MEPS model and defines BGF events via $\hat{s} > y_{\text{min}} \cdot W^2$. The parameter y_{min} is then varied between 0.0025 and 0.01 to study its influence on the result. The H1 and ZEUS results [16] agree well with each other, but yield different size systematic errors (figure 3). The ZEUS errors receive large contributions from the y_{min} variation. The rise of the measured gluon density towards small x can be described by a LO gluon density [18] following the DGLAP (Dokshitzer-Gribov-Lipatov-Altarelli-Parisi) [21] equations. The data are also consistent with the indirect determination of $g(x_g, Q^2)$ from the scaling violations of F_2 [19], providing a non-trivial test of QCD.

2.3. Open Points

Lack of understanding of parton showers close to the remnant (model dependent corrections, failure of NLO calculations) currently prevents the α_s analysis to make full use of the large statistics data at $Q^2 < 100 \text{ GeV}^2$.

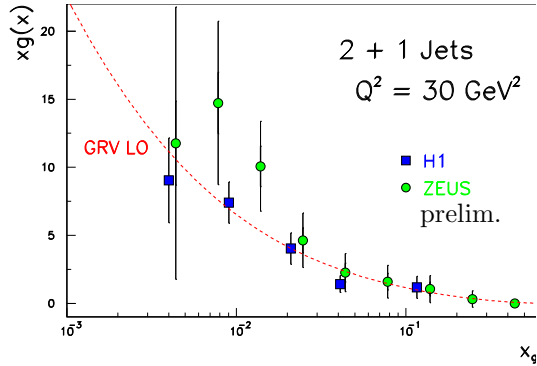


Figure 3. The gluon density in the proton, determined in leading order (LO) from the rate of 2+1 jet events. Shown are data from H1 and ZEUS, compared to the LO GRV [18] gluon density parametrization.

Though increasing HERA luminosity will allow the α_s analysis to be restricted to higher Q^2 to reduce uncertainties, the understanding of the forward region remains a challenge.

So far the α_s measurements rely solely upon the JADE algorithm, being the only algorithm for which NLO jet cross sections are calculated [22]. NLO calculations for other algorithms, such as the cone [23] or the theoretically preferred k_T [24] algorithm are desirable. Such a program, which would also be able to calculate event shape variables like energy-energy correlations, Thrust, etc., is being worked upon by D. Graudenz, but results cannot be expected in a short term. Theoretical uncertainties could also be reduced by resumming higher order corrections.

The validity of corrections from hadronic to partonic final states, defined either in LO or NLO, need to be checked with models based upon different parton shower and hadronization schemes. Unfortunately, a MC generator incorporating the QCD matrix elements beyond LO is missing.

The gluon density has so far been determined in LO. A method allowing a measurement in NLO is presently under study [12].

How can α_s be determined consistently, considering it is input for the evolution of parton densities which are used in the analysis [25]?

3. Novel QCD dynamics

The observed strong rise of the structure function F_2 towards small x [20] has caused much debate on whether the QCD evolution of the parton densities can still be described by the conventional DGLAP [21] equations, or whether the HERA data extend into a new regime at small x where the dynamics is governed by the BFKL (Balitsky-Fadin-Kuraev-Lipatov) [26] equation. It would be extremely interesting to test QCD in such

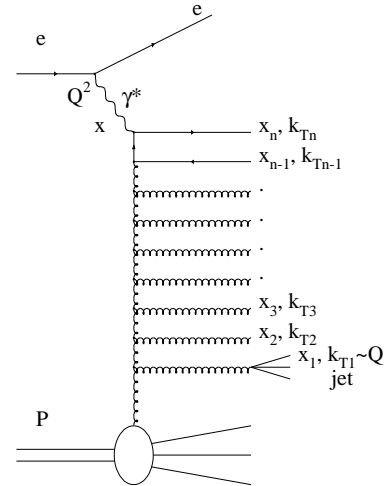


Figure 4. Parton evolution in the ladder approximation. The selection of forward jets in DIS events is illustrated.

a new regime. While the rise is consistent with the expectation from BFKL dynamics, it can however also be described by a DGLAP evolution [27]. At lowest order the BFKL and DGLAP equations resum the leading logarithmic $(\alpha_s \ln 1/x)^n$ or $(\alpha_s \ln(Q^2/Q_0^2))^n$ contributions respectively. In this approximation the leading diagrams are of the ladder type (figure 4). The leading log DGLAP ansatz corresponds to a strong ordering of the transverse momenta k_T (w.r.t. the proton beam) in the parton cascade ($Q_0^2 \ll k_{T1}^2 \ll \dots k_{Tj}^2 \ll \dots Q^2$), while there is no such ordering in the BFKL ansatz ($k_{Tj}^2 \approx k_{Tj+1}^2$) [28]. Measurements on the hadronic final state emerging from the cascade therefore offer another handle to search for signatures of the BFKL behaviour. They are compared to analytical calculations as well as to the QCD models MEPS and CDM. The CDM description of gluon emission is similar to that of the BFKL evolution, because the gluons emitted by the dipoles do not obey strong ordering in k_T [29]. The MEPS model with its leading log parton shower is based upon DGLAP dynamics, and the emitted partons are thus ordered in k_T .

3.1. Transverse Energy Production

As a consequence of the strong k_T ordering the DGLAP evolution is expected to produce less transverse energy E_T in a region between the current region and the proton remnant than the BFKL evolution [30]. H1 and ZEUS have measured the flow of transverse energy in the laboratory frame as a function of pseudorapidity $\eta = -\ln \tan(\theta/2)$, where θ is the angle of the energy deposition w.r.t the proton beam axis [31, 32, 33]. The measurements are made for varying ranges in x ($2 \cdot 10^{-4} < \langle x \rangle < 5 \cdot 10^{-3}$) and Q^2 ($7 \text{ GeV}^2 < \langle Q^2 \rangle <$

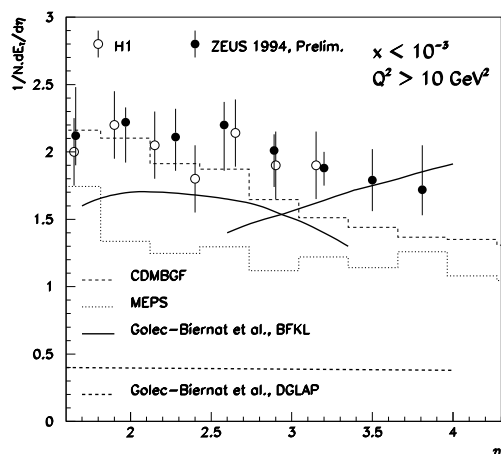


Figure 5. Transverse energy flow in the forward region at H1 [31] and ZEUS [32] for $x < 10^{-3}$. The proton direction is to the right. The calorimeter acceptances end at η around 3.5. The data are compared to the CDM (here labelled CDMBGF) and MEPS models and to partonic calculations based upon the DGLAP and BFKL equations [30].

30 GeV² and agree well between the experiments [32].

The E_T flows for large x and Q^2 are reasonably well described by MEPS and CDM. For smaller x and Q^2 both models predict a more pronounced enhancement in the current fragmentation region than is seen in the data. Between the current system and the proton remnant (the lab. forward region), the data are reasonably well described by the CDM, while the MEPS model produces too little E_T [31, 32]. This intermediate region is expanded in figure 5, because there perturbative calculations, based either on DGLAP or on BFKL dynamics, are available [30]. The BFKL calculation comes out close to the data, while the DGLAP calculation predicts much less E_T . However, the non-perturbative hadronization phase is missing in these calculations.

H1 has determined the average E_T , measured centrally in the CMS as a function of x and Q^2 (figure 6). They find an increase of $\langle E_T \rangle$ with decreasing x , which is a characteristic BFKL prediction [30]. The data are in agreement with the BFKL calculation [34], if one assumes an E_T contribution from hadronization of about 0.4 GeV per unit rapidity (independent of x). That estimate is taken from the CDM, which agrees with the BFKL calculation at the parton level.

The apparent failure of the MEPS model has caused many questions about its ingredients: the way the parton shower is “matched” to the matrix element, the colour connection between the current and the remnant system and its effect upon hadronization, and the remnant fragmentation itself which is little tested. It seems that re-arranging colour configurations

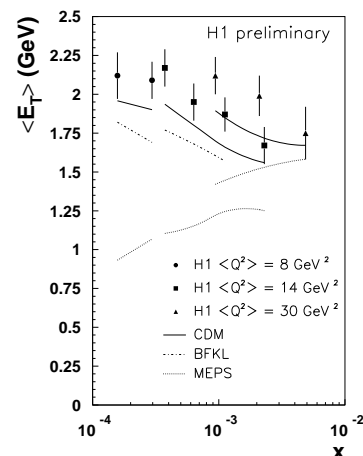


Figure 6. Transverse energy $\langle E_T \rangle$ per unit of pseudorapidity η^* as a function of x for three different values of Q^2 , measured centrally at $\eta^* = 0$ in the CMS (corresponding to the lab. forward region). The data are compared to the CDM and MEPS models including hadronization, and to the BFKL calculation (no hadronization).

can produce enough E_T through hadronization to compensate the E_T deficit in the DGLAP cascade of the MEPS model [35]. A MEPS version thus modified should be available soon for detailed testing. The flexibility in the hadronization modelling presently precludes unambiguous tests of the DGLAP evolution through E_T measurements. For the same reasons the intriguing success of the CDM without k_T ordering may be fortuitous. A MC model invoking explicitly the BFKL evolution, currently being developed by K. Golec-Biernat et al., would help interpreting the data. In any case, the E_T data provide important input for QCD phenomenology.

3.2. Forward Jets

At present strong conclusions upon the validity of the BFKL or DGLAP parton evolutions at small x from the E_T measurements are hampered by the uncertainties about hadronization. Jet production should be less affected by hadronization. A signature for BFKL dynamics proposed by [36] is the production of “forward jets” with $x_{\text{jet}} = E_{\text{jet}}/E_p$, the ratio of jet energy and proton beam energy, as large as possible, and with transverse momentum $k_{T\text{jet}}$ close to Q in order to reduce the phase space for the k_T ordered DGLAP evolution (see figure 4). An enhanced rate of events with such jets is thus expected in the BFKL scheme [36, 37]. The experimental difficulty is to detect these “forward” jets which are close to the beam hole in proton direction.

The rate of forward jets measured by H1 [38, 33] (figure 7) is larger at low x than at high x . This

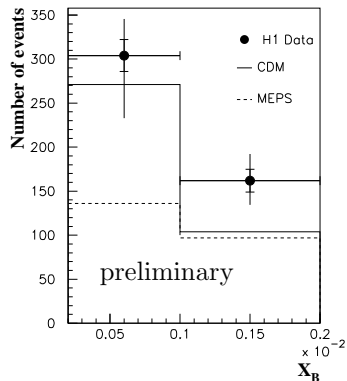


Figure 7. The rate of forward jets (selected with $x_{\text{jet}} > 0.025$, $0.5 < k_{T\text{jet}}^2/Q^2 < 4$ and $k_{T\text{jet}} > 5$ GeV) in the kinematic range $2 \cdot 10^{-4} < x < 2 \cdot 10^{-3}$ and $Q^2 \approx 20$ GeV². The measurement is compared to the CDM and MEPS models.

is expected from BFKL calculations, in contrast to calculations without BFKL ladder [37, 39]. The behaviour of the data is better represented by the CDM than by the MEPS model. However, neither of them describe the energy spectrum of the observed jets correctly, and the model predictions for the jet rates are thus cut dependent [38, 33]. The analysis of a larger statistics sample should allow more firm conclusions.

ZEUS has measured an inclusive jet cross section $d\sigma/dE_{T\text{jet}}$ in the Breit frame [38]. Many more jets are found in the target region with a harder $E_{T\text{jet}}$ spectrum than in the current region, reflecting the differences in phase space in the two regions. The current region data are reasonably well described by the CDM and MEPS models. In the target region however there is a substantial excess of jets over the model predictions, which can be linked with an excess of $2 + 1$ jet events [38]. In the laboratory frame this excess is located in the forward region at angles $\theta_{\text{jet}} < 20^\circ$ (figure 8).

The data on jet production in the forward region (lab. frame), or the target region (Breit frame) certainly pose a challenge to theory. So far cross sections are calculated [37, 39] only for partons, while experiments measure hadron jets. This gap has to be bridged from both sides to allow a strictly valid comparison.

3.3. Jet correlations

Apart from calculations of forward jet rates, Del Duca [39] discussed angular correlations for forward jets. If a BFKL ladder is inserted in between the electron-photon vertex and the forward jet, the angular correlation between the forward jet and the electron imposed by momentum conservation is relaxed. Such angular decorrelation could be another footprint of BFKL dynamics. The fact that 4% of the H1 forward jet events contain a second forward jet [38] opens another route of investigation, namely correlations between such

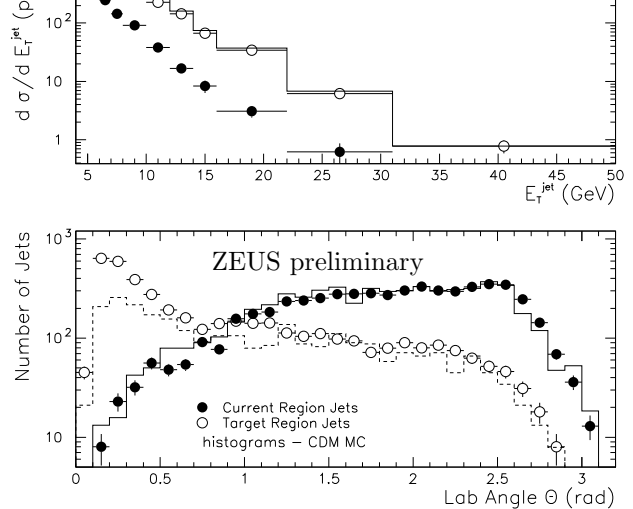


Figure 8. The laboratory angular distribution of jets detected either in the Breit current or target hemisphere.

jets. If these jets can be identified with gluons emitted from the ladder, it would be possible to check the parton ordering directly.

3.4. Dipole emission

An interesting ansatz to calculate final state observables was presented by R. Peschanski [42]. The starting point is onium-onium scattering [43] with onium wave functions which can be derived from QCD. Such a reaction is analogous to an interaction of the current system with the remnant system in DIS. Radiation is treated in the dipole picture, leading to a copious production of dipoles in the central rapidity region of the interaction. Once such an ansatz yields quantitative predictions, it could be tested in DIS, e.g. with E_T flow measurements.

Bo Andersson [40] discussed DIS final states in terms of a chain of radiating colour dipoles, and its connection with the Ciafaloni-Catani-Fiorini-Marchesini ansatz [41]. In principle this model could provide a complete picture of the hadronic final state in DIS. The implementation in the Ariadne [5] MC generator is in progress to allow detailed predictions.

3.5. QCD Instantons

The standard model contains processes which cannot be described by perturbation theory, and which violate classical conservation laws like baryon and lepton number in the case of the electroweak sector and chirality for the strong interaction [44]. Such anomalous processes are induced by instantons [45]. At HERA, QCD instantons may lead to observable effects in the hadronic final state in DIS [46, 47], which were discussed by F. Schrempp. The instanton should decay isotropically into a high multiplicity state of gluons and all quark flavours simultaneously which are kinematically allowed. A MC program to simulate instanton events has become available [48]. Due to the isotropic decay, one expects a densely populated region in rapidity, other than the current jet, which is isotropic

in azimuth. The presence of strangeness and charm could provide an additional signature. However remote the a priori chances to see such signals may appear, here is a chance for a major discovery at HERA!

4. Charged Particle Spectra

The H1 and ZEUS measurements of inclusive charged particle spectra [49] are performed either in the Breit frame or in the CMS. In the Breit frame in- and outgoing quark have equal but opposite sign momenta $Q/2$ (QPM picture), and in e^+e^- annihilation the outgoing quark and antiquark have equal but opposite momenta $\sqrt{s}/2 = Q/2$. Due to this similarity it is interesting to compare particle spectra in the Breit current hemisphere in DIS with e^+e^- data. DIS experiments have the advantage over e^+e^- experiments that they cover a large span in Q , presently from 3 GeV to 50 GeV, in a single experiment. The current mean charged multiplicity at HERA rises $\sim \ln Q$ within errors, and agrees with e^+e^- data (divided by 2) where they overlap [50, 49].

Colour coherence should lead to a suppression of soft gluon emission. The HERA data [50, 49] on the scaled charged particle momentum distribution $\ln 1/x_F$ with $x_F = 2 \cdot p/Q$ exhibit the expected hump backed plateau [51], the evolution of which with Q is in agreement with the assumption of colour coherence. However, like in e^+e^- annihilation, this behaviour can also be mimicked through the Lund string fragmentation [49].

The scaled momentum spectrum of x_F in the CMS, where the particle longitudinal momenta p_z are divided by the maximal possible momentum, $x_F = 2 \cdot p_z/W$, are shown in figure 9 for the current region (the target region is not observed). Comparing HERA data at $W \approx 120$ GeV [31, 49] with fixed target data at $W = 14$ and 18 GeV [53, 52], significant scaling violations are observed, in agreement with QCD expectations: the large value of W at HERA results in a large phase space for QCD radiation, softening the x_F spectrum w.r.t. data at lower W . It can be expected that such data will be used to extract α_s in the future.

The effect of QCD radiation is clearly seen in the “seagull plot” (figure 10), where the mean transverse momenta p_T^2 squared of the particles is plotted as a function of x_F . As a consequence of increased QCD radiation, much larger p_T^2 are observed at HERA [31, 49] than at EMC [53] at smaller W , again in agreement with QCD expectation. ZEUS has also compared DIS events with and without a large rapidity gap [54] in this respect [49]. Much smaller p_T^2 than in normal DIS events are observed in events with a large rapidity gap, thought to stem from diffractive processes and accounting for approximately 10% of the total sample [54]. This indicates that the scale governing radiation is much smaller than W for rapidity gap events.

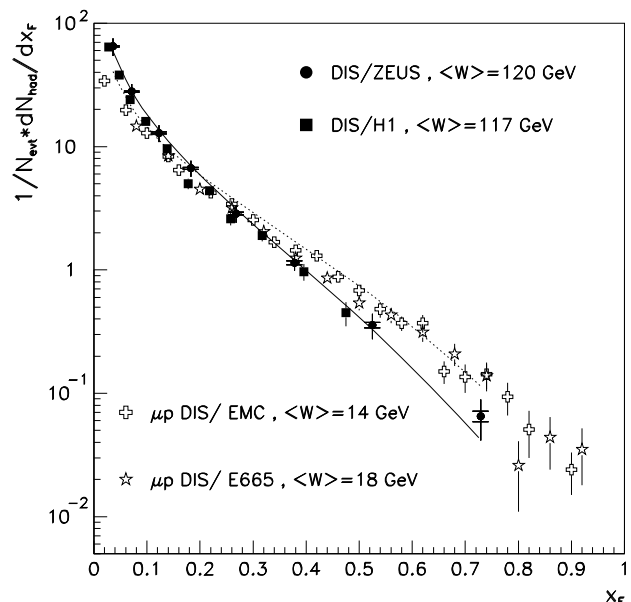


Figure 9. The x_F spectra measured at HERA compared with the QPM (dotted line) without QCD radiation, the MEPS model (full line), and with fixed target DIS data at lower W .

5. Conclusion

Two complementary approaches to the HERA data can be distinguished. In one approach, one tries to identify a region which is “well understood”, meaning that the observation agrees with the theory and the models. Under this condition, the data can be interpreted in the framework of the theory, and physical quantities which are defined within the theory can be extracted. The measurements of α_s and $g(x_g, Q^2)$ fall into this category. However, we have also seen data which are not yet understood theoretically, namely hadron and jet production in the forward region. Such data currently pose a challenge to the theory, and experimentalists should make every effort to provide theory with solid data to work with.

Acknowledgements

I would like to thank my fellow conveners, A. Doyle and G. Ingelman, for the pleasant cooperation, the organizers of the workshop for their efficient support and the participants of the session for their contributions and inspiring discussions in the working group.

References

- [1] J. Bartels and J. Feltesse, Proc. of the Workshop on Physics at HERA, Hamburg 1991, eds. W. Buchmüller and G. Ingelman, vol. 1, p. 131;
E.M. Levin, Proc. QCD – 20 Years Later, Aachen 1992, eds. P.M. Zerwas, H.A. Kastrup, vol. 1, p. 310.

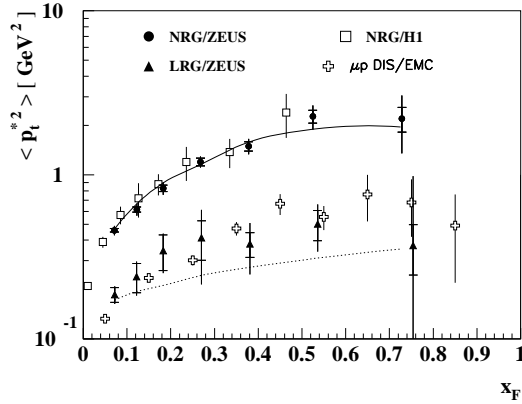


Figure 10. The seagull plot. Shown are the mean transverse momenta squared ($\langle p_T^2 \rangle$) as a function of x_F in the CMS for HERA data with and without a rapidity gap (LRG/NRG) compared to the QPM prediction (dotted line) and the MEPS model (full line), and to EMC data at lower W .

- [2] H1 Collab., I. Abt et al., DESY 93-103 (1993); ZEUS Collab., M. Derrick et al., Phys. Lett. B293 (1992) 465.
- [3] G. Ingelman, Proc. of the Workshop on Physics at HERA, Hamburg 1991, eds. W. Buchmüller and G. Ingelman, vol. 3, p. 1366.
- [4] G. Gustafson, Ulf Petterson, Nucl. Phys. B306 (1988); G. Gustafson, Phys. Lett. B175 (1986) 453; B. Andersson, G. Gustafson, L. Lönnblad, Ulf Petterson, Z. Phys. C43 (1989) 625.
- [5] L. Lönnblad, Comp. Phys. Comm. 71 (1992) 15.
- [6] T. Sjöstrand, Comp. Phys. Comm. 39 (1986) 347; T. Sjöstrand and M. Bengtsson, Comp. Phys. Comm. 43 (1987) 367; T. Sjöstrand, CERN-TH-6488-92 (1992).
- [7] G. Marchesini, B.R. Webber, G. Abbiendi, I.G. Knowles, M.H. Seymour and L. Stanco, Comp. Phys. Comm. 67 (1992) 465.
- [8] M. Seymour, Lund preprint LU-TP-94-12 (1994).
- [9] B. Webber, these proceedings.
- [10] B.R. Webber, Nucl. Phys. B238 (1984) 492.
- [11] JADE Collab., W. Bartel et al., Z. Phys. C33 (1986) 23.
- [12] D. Graudenz, these proceedings.
- [13] H1 Collab., T. Ahmed et al., Phys. Lett. B346 (1995) 415.
- [14] D. Graudenz, Projet 4.13 manual, CERN-TH 7420/94.
- [15] ZEUS Collab., M. Derrick et al., DESY 95-016.
- [16] G. Grindhammer, these proceedings.
- [17] H1 Collab., S. Aid et al., DESY 95-086 (1995).
- [18] M. Glück, E. Reya, A. Vogt, U. Dortmund preprint DO-TH-94-24.
- [19] ZEUS Collab., M. Derrick et al., Phys. Lett. B345 (1995) 576; H1 Collab., S. Aid et al., DESY 95-081 (1995).
- [20] ZEUS Collab., M. Derrick et al., Z. Phys. C65 (1995) 379; H1 Collab., T. Ahmed et al., Nucl. Phys. B439 (1995) 471.
- [21] Yu. L. Dokshitzer, Sov. Phys. JETP 46 (1977) 641; V.N. Gribov and L.N. Lipatov, Sov. J. Nucl. Phys. 15 (1972) 438 and 675; G. Altarelli and G. Parisi, Nucl. Phys. 126 (1977) 297.
- [22] D. Graudenz, Phys. Lett. B256 (1991) 518; Phys. Rev. D49 (1994) 3291; T. Brodtkorb, J.G. Körner, Z. Phys. C54 (1992) 519; T. Brodtkorb, E. Mirkes, U. Wisconsin preprint MAD/PH/820 (1994).
- [23] B. Webber, J. Phys. G19 (1993) 1567.
- [24] S. Catani, Y.L. Dokshitzer, B. Webber, Phys. Lett. B285 (1992) 291.
- [25] A. Vogt, DESY 95-068.
- [26] E.A. Kuraev, L.N. Lipatov and V.S. Fadin, Sov. Phys. JETP 45 (1972) 199; Y.Y. Balitsky and L.N. Lipatov, Sov. J. Nucl. Phys. 28 (1978) 282.
- [27] A.J. Askew, J. Kwieciński, A.D. Martin and P.J. Sutton, Phys. Lett. B325 (1994) 212.
- [28] J. Bartels, H. Lotter, Phys. Lett. B309 (1993) 400; A. Mueller, Columbia preprint CU-TP-658 (1994).
- [29] A. H. Mueller, Nucl. Phys. B415 (1994) 373; L. Lönnblad, Z. Phys. C65 (1995) 285 and CERN-TH/95-95.
- [30] J. Kwieciński, A.D. Martin, P.J. Sutton and K. Golec-Biernat, Phys. Rev. D50 (1994) 217. K. Golec-Biernat, J. Kwieciński, A.D. Martin and P.J. Sutton, Phys. Lett. B335 (1994) 220.
- [31] H1 Collab., I. Abt et al., Z. Phys. C63 (1994) 377.
- [32] T. Haas, these proceedings.
- [33] H1 Collab., S. Aid et al., DESY-95-108.
- [34] calculation by P. Sutton on the basis of [30].
- [35] G. Ingelman, these proceedings.
- [36] A.H. Mueller, Nucl. Phys. B (Proc. Suppl.) 18C (1990) 125; J. Phys. G17 (1991) 1443.
- [37] J. Kwieciński, A.D. Martin, P.J. Sutton, Phys. Rev. D46 (1992) 921.
- [38] A. DeRoeck, these proceedings.
- [39] V. Del Duca, these proceedings.
- [40] B. Andersson, these proceedings
- [41] M. Ciafaloni, Nucl. Phys. B296 (1988) 49; S. Catani, F. Fiorani and G. Marchesini, Phys. Lett. B234 (1990) 339; Nucl. Phys. B336 (1990) 18.
- [42] R. Peschanski, these proceedings.
- [43] A.H. Mueller, Nucl. Phys. B415 (1994) 373; ibid. B437 (1995) 107. A.H. Mueller and B. Patel, Nucl. Phys. B425 (1994) 471. A. Bialas and R. Peschanski, Saclay-Orsay preprint T95/032, LPTHE-95/29.
- [44] G. 't Hooft, Phys. Rev. Lett. 37 (1976) 8; Phys. Rev. D14 (1976) 3432.
- [45] A. Belavin, A. Polyakov, A. Schwarz and Yu. Tyupkin, Phys. Lett. B59 (1975) 85.
- [46] A. Ringwald, Nucl. Phys. B330 (1990) 1; O. Espinosa, Nucl. Phys. B343 (1990) 310.
- [47] A. Ringwald and F. Schrempp, DESY 94-197.
- [48] M. Gibbs, A. Ringwald and F. Schrempp, work presented by F. Schrempp at this workshop.
- [49] N. Pavel, these proceedings.
- [50] ZEUS Collab., M. Derrick et al., DESY 95-007; H1 Collab., I. Abt et al., DESY 95-072.
- [51] Y. Dokshitzer, V. Khoze, A. Mueller and S. Troyan, "Basics of Perturbative QCD", Gif-sur-Yvette, France (1991).
- [52] E665 Collab., M.R. Adams et al., Phys. Rev. D50 (1994) 1836.
- [53] EMC Collab., J. Ashman et al., Z. Phys. C52 (1991) 361.
- [54] ZEUS Collab., M. Derrick et al., Phys. Lett. B315 (1993) 481; H1 Collab., T. Ahmed et al., Nucl. Phys. B429 (1994) 477.